Instability and dynamics of EHD flow with unipolar and bipolar charge injection in an annulus

D. V. Fernandes[*] H. D. Lee[*] and Y. K. Suh[*+]

[*]Dong-A University, Busan, South Korea, [+]yksuh@dau.ac.kr

ABSTRACT

Electrohydrodynamic (EHD) flows of dielectric liquid are ubiquitous in engineering applications such as heat transfer, pumping and mixing. Present study describes the numerical simulation of EHD flow instability in the annular gap between two concentric circular cylinders with unipolar and bipolar charge injection. The Nernst-Planck equations governing the charge density transport, the Poisson equation for the electric potential and the Navier-Stokes equations for the fluid flow are solved numerically using the finite volume method. The developed code was validated by comparing values of T_C , the critical parameter for the onset of electro-convection, with those given by a linear instability analysis. We have found that the outer-injection case is more stable than the inner injection, but it becomes more unstable with increase of the inner cylinder size (r_i), whereas the trend is opposite in the inner-injection case. The wave number characterizing the vortical flow increases with r_i in agreement with the linear analysis. We identify in a parameter space the stable hydrostatic state and the electro-convection state. The electro-convection state is again divided into three regimes; stationary, oscillatory and chaotic. For the bipolar injection case we observed travelling-wave-type vortical flows at a certain parameter set. The wave number of the travelling-wave vortical flow shows regular fluctuations for certain parameter set, which was confirmed from the beat like variations in the fluid velocity.

Keywords: electrohydrodynamic flow, charge injection, stability, annulus, electro-convection

1 INTRODUCTION

The science of electric-field-induced fluid flow i.e., electrohydrodynamics (EHD) has fascinated many researchers involved in fluid dynamics from quite a long ago. EHD flow plays a key role in many technological applications, such as EHD pumps [1-2], electric power industry [3], electronic cooling [4], heat exchangers [5], and electrorheological devices, e.g., brakes, actuators, etc [6].

There is fundamental difference in the mechanism of EHD flow between the aqueous (polar) solution and the dielectric (non-polar) liquid. The aqueous solution contains free ions, and the bulk is neutralized while the electric double layer (EDL) adjacent to walls is charged by the accumulation of counter ions. External field then drives the fluid parallel to the walls leading to the electroosmotic flows. On the other hand, for the dielectric liquid case, the EDL effect is weak and the bulk is charged through the charge injection from electrode surfaces and/or through the dissociation of ion pairs subjected to a high electric field under the Onsager effect [7]. Though the aqueous solutions or electrolytes have free charges being able to cause strong EHD flow, they suffer from the problem of electrode degradation through electrolysis. The dielectric or low-conductivity liquids on the other hand can exhibit the same level of EHD flow velocity as the aqueous solutions at very high electric field but free of such problem.

It has been found that at high electric field the charge injection becomes dominant over the dissociation effect. The charge injection is an electrochemical process where neutral species undergo reduction or oxidation reactions at the electrode surface. It is also possible to have a controlled injection of charge from metallic electrodes by coating them with radioactive paints or varnishes or electro-dialytic membranes [8].

In this study we have performed numerical simulations of 2D charge-transport and fluid-flow equations for dielectric liquid between two perfectly conducting coaxial cylinders under autonomous unipolar/bipolar charge injection. We have investigated the effect of injection strength and cylindrical aspect ratio on the onset of electroconvection. To validate our code, we compared our results with the ones given from the linear instability analysis in terms of the critical stability parameter values for the onset of electro-convection.

2 MATHEMATICAL MODEL

The physical domain consists of an annulus made of perfectly conducting inner solid cylinder of radius r_i and outer hollow cylinder of inner radius r_o . The annulus is filled with an incompressible dielectric liquid of density ρ , permittivity ε , kinematic viscosity ν , diffusivity D and charge carrier mobility K . An electric potential difference of ϕ_0 is applied between the two cylinders.

We present the mathematical model in dimensionless form by scaling the governing equations using the following reference quantities; $d = r_o - r_i$ for the spatial

coordinates, ϕ_0 for the potential, $U_0 = K\phi_0/d$ for the velocity, $q_0 = \varepsilon\phi_0/d^2$ for the charge density, $t_0 = d/U_0$ for the time, and $p_0 = \rho U_0^2$ for the pressure.

Gauss law:

$$\nabla \cdot \mathbf{E} = q \tag{1}$$

Charge conservation:

$$\frac{\partial f}{\partial t} + \nabla \cdot \left[(\mathbf{u} + \mathbf{E}) f \right] = \frac{1}{Pe} \nabla^2 f \tag{2}$$

$$\frac{\partial g}{\partial t} + \nabla \cdot \left[(\mathbf{u} - \mathbf{E}) g \right] = \frac{1}{Pe} \nabla^2 g \tag{3}$$

Navier-Stokes equations:

$$\nabla \cdot \mathbf{u} = 0 \tag{4}$$

$$\frac{\partial \mathbf{u}}{\partial t} + (\mathbf{u} \cdot \nabla)\mathbf{u} + \nabla p = \frac{1}{\mathrm{Re}} \nabla^2 \mathbf{u} + M^2 q \mathbf{E} \tag{5}$$

where $\mathbf{E} = -\nabla\phi$ is the electric field, q the space charge density, f the cation concentration, g the anion concentration, $\mathbf{u}$ the fluid velocity vector, p the pressure and ϕ the electric potential. The dimensionless parameters; $Pe = Sc\,\mathrm{Re}$ is the Péclet number, $\mathrm{Re} = T/M^2$ the electrical Reynolds number, $Sc = \nu/D$ the Schmidt number, $T = \varepsilon\phi_0/(\rho\nu K)$ the stability parameter, and $M = \sqrt{\varepsilon/(\rho K^2)}$ the mobility parameter.

In case of unipolar injection, charge is injected from one of the cylindrical electrodes and discharged at the other. Without loss of generality, we assume that the injected charge is positive. Thus for unipolar injection $q = f$ and Eq. 3 is not required to be solved. For the bipolar case complete model (Eqs. 1-5) need to be solved and the space charge density is given by $q = f - g$.

We assume autonomous charge injection, that is, injector electrode is set at a constant charge density q_s. The electric potential ϕ on the anode is set at 1 while that on the cathode is set at 0. As usual, no-slip and impermeable boundary condition ($\mathbf{u} = 0$) is applied on both the electrode surfaces.

3 REULTS AND DISCUSSION

The governing equations are solved numerically using finite-volume method on a uniform staggered-grid system. The numerical code is validated by comparing the results of onset of electro-convection with those obtained from the linear instability analysis. The numerical solutions are obtained by fixing Schmidt number at $Sc = 10,000$ and the electric Reynolds number at $\mathrm{Re} = 1$; then Pe is fixed automatically at $Pe = 10,000$. For a given set of the inner cylinder radius r_i and the injection strength q_s, we performed numerical simulations to find a critical stability parameter T_C, at which the one-dimensional conduction state becomes unstable leading to electro-convection. Near the onset, the electro-convection develops into a regular stationary vortex structure, composed of multiple pairs of counter-rotating vortices.

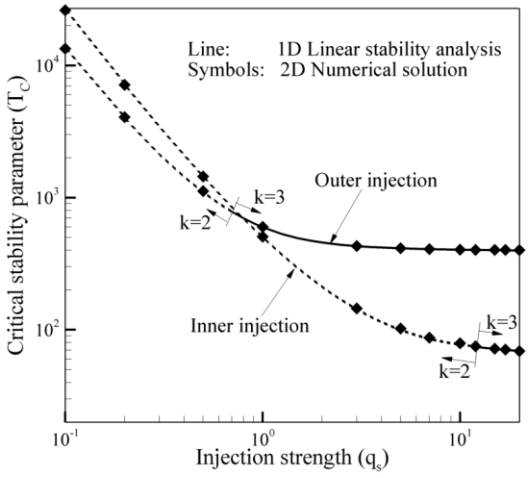

Figure 1: Effect of the injection strength on T_C at $r_i = 0.1$.

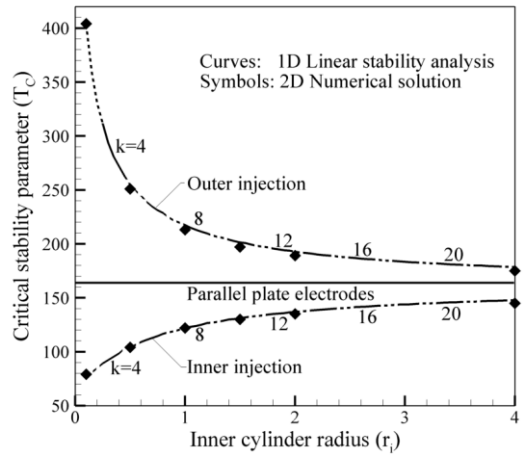

Figure 2: Effect of r_i on T_C at $q_s = 10$.

Figure 1 shows comparison of T_C data obtained from the 2D numerical simulations and the ones given from the linear instability analysis for different q_s at $r_i = 0.1$. Exact matching between the two results shows the validity of the numerical code. In general, stronger injection leads to more unstable situation, as expected. It is interesting to note that, while the instability of the inner injection occurs at T smaller than that of the outer injection for q_s above 0.8, it occurs at a larger T for q_s below 0.8. This implies that the inner injection tends to be more unstable at stronger injection than the outer injection.

Figure 2 shows the variation of T_C with the inner cylinder radius r_i for both inner and outer injection. We can see that the 2D numerical simulations results are in good agreement with those given by the 1D linear instability analysis. Also we can notice that for inner injection T_C increases with r_i, whereas for outer injection it decreases with r_i. And as r_i tends to infinity, T_C asymptotically approaches to the value for the parallel plate case.

3.1 Non-linear electro-convection

Simulations are carried out for a strong injection ($q_s = 10$) at T beyond T_C up to 1000 to identify various instability regimes. Figure 3 shows the map (r_i, T) of solution regimes for the inner injection. We can distinguish hydrostatic and electro-convection regimes. The electro-convection region is divided into three subregions: stationary, oscillatory and chaotic. The stationary electro-convection occurs with definite number of vortex pairs having their vortex centers fixed at particular locations. In the oscillatory electro-convection, the flow velocity shows sinusoidal variation in time. In the chaotic regime, the flow becomes random and complex with fluctuating waves.

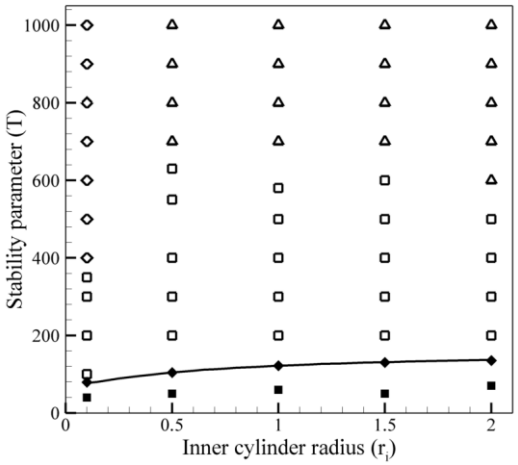

Figure 3: Map of flow patterns for inner injection; curve, 1D linear instability analysis; symbols, 2D numerical solution. Symbol classification: ■, 1D hydrostatic regime; ♦, critical; □, stationary electro-convection; ◊, oscillatory electro-convection; Δ, chaotic electro-convection.

Figure 4 shows typical solutions of stationary electro-convection of regular vortical flow obtained at $r_i = 0.1$, $q_s = 10$ and $T = 100$. We can see two pairs of vortices and two charged plumes emanating from the injection electrode. The azimuthal location of the plumes is of course random, but once the plumes are built they remain stationary there.

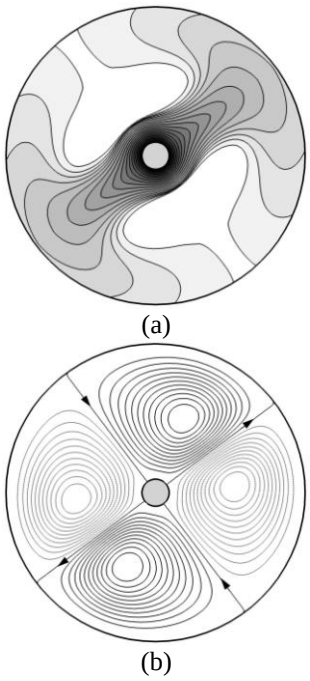

Figure 4: Typical stationary electro-convection for inner injection at $r_i = 0.1$, $q_s = 10$ and $T = 100$; (a) contours of charge density and (b) streamlines.

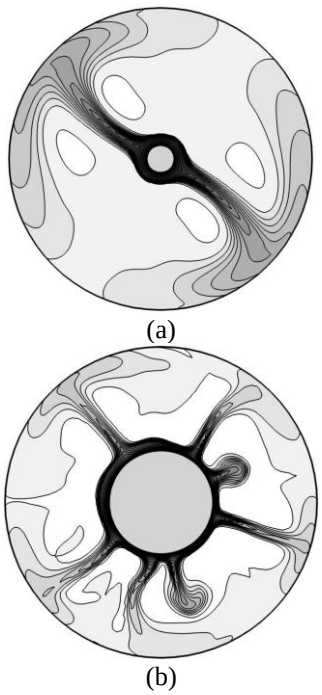

Figure 5: Instantaneous charge-density contours (a) typical oscillatory electro-convection for inner injection at $r_i = 0.1$, $q_s = 10$, and $T = 500$ and (b) typical chaotic electro-convection at $r_i = 0.5$, $q_s = 10$ and $T = 1000$.

Figure 5 shows the instantaneous charge density contours of an oscillatory flow and a chaotic flow. The

instantaneous charge-density contours of typical chaotic flow shows the creation of new charged plumes. As the new charged plumes grow, either the neighboring plumes become weaker and subsequently disappear or the new plume moves closer to one of the neighbors and merges with it. The charged plumes exhibit random twisting and bending motion as they develop. Thus such process of creation and subsequent disappearance of charged plumes seems to make the fluid flow chaotic.

3.2 Electro-convection with bipolar injection

Electro-convection due to bipolar injection is studied by solving Eqs. (1)–(5) numerically. We considered strong injection of cations $q_{si} = 10$ from the inner electrode, while anion injection strength at the outer electrode q_{so} is varied from 0.1 to 5.

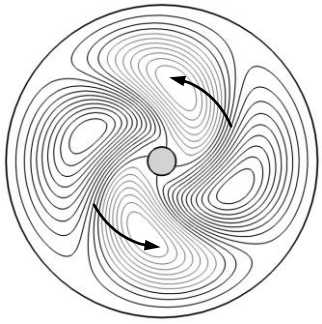

Figure 6: Rotating vortical-flow pattern for bipolar injection at $T = 200$ and $r_i = 0.1$ when $q_{si} = 10$ and $q_{so} = 2$

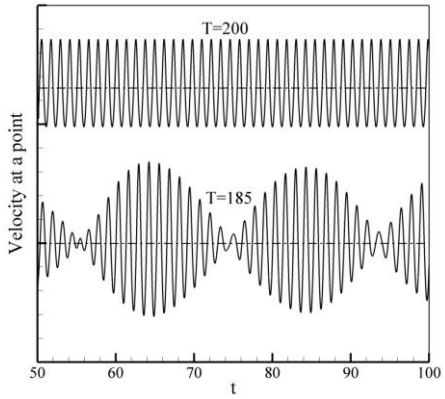

Figure 7: Time variation of velocity at a point in the domain at $T = 185$ and $T = 200$, for a bipolar injection case.

It is found that for a fixed q_{si} electro-convection becomes more stable (T_C increases) as the q_{so} increases. The EHD flow in case of bipolar injection is generally chaotic in nature. But for a certain parameter set electroconvection shows regularly rotating vortical-flow structure as shown in Fig. 6. The wave number of the traveling-wave vortical flow shows regular fluctuations for certain parameter set, which can be seen from the beat like variations in the fluid velocity, as observed in Fig. 7.

4 CONCLUSIONS

In this study we performed two-dimensional numerical simulations of EHD flow induced by autonomous unipolar/bipolar charge injection in an annular geometry filled with dielectric liquid. We computed critical stability parameter T_C for the onset of electro-convection at various injection strength q_s and cylindrical aspect ratio (related to r_i), and the results were in good agreement with the ones given from linear stability analysis. We found that the stronger injection leads to more unstable situation. And also the outer injection produces the onset of instability at T smaller than the inner injection for weak injection and vice versa for strong injection. As for the effect of curvature, we confirmed that as r_i tends to infinity T_C asymptotically approaches to the value for the parallel plate case.

The parametric study with inner injection shows that the electro-convection regime can be divided into stationary, oscillatory and chaotic regimes. The oscillatory electroconvection is however observed only for inner injection at $r_i = 0.1$. For the bipolar injection, flow is generally chaotic, but turns to regular rotating vortical-flow for a certain parameter set.

ACKNOWLEDGMENTS

This work was supported by NRF grant No. 2009-0083510 through Multi-phenomena CFD Engineering Research Center and by the Human Resources Development of the Korea Institute of Energy Technology Evaluation and Planning (KETEP) grant funded by the Korea government Ministry of Knowledge Economy (No. 20114030200030).

REFERENCES

[1] R. Hanaoka, I. Takahashi, S. Takata, T. Fukami, and Y. Kanamaru, IEEE Trans. Dielectr. Electr. Insul., 16, 440, 2009.
[2] W. Kim, J. C. Ryu, Y. K. Suh, and K. H. Kang, Appl. Phys. Lett., 29, 224102, 2011.
[3] J. M. Cabalerio, T. Paillat, O. Moreau, and G. Touchard, IEEE Trans. Ind. Appl., 45, 597, 2009.
[4] P. Kazemi, P. R. Selvaganapathy, and C. Y. Ching, IEEE Trans. Dielectr. Electr. Insul., 16, 483, 2009.
[5] J. Cotton, A. J. Robinson, M. Shoukri, and J. S. Chang, Int. J. Heat Mass Transfer, 48, 5563, 2005.
[6] T. Hao, Electrorheological suspensions, Adv. Colloid Interface Sci., 97, (2002) 1-35.
[7] A. S. Dukhin and P. J. Goetz, J. Electroan. Chem., 588, 44, 2006.
[8] N. Agrait and A. Castellanos, Phys. Fluids A, 2, 37, 1990.